Electronic Supplementary Material (ESI) for Journal of Materials Chemistry A.

Mo-doped LiV_3O_8 nanorod-assembled nanosheets as a high performance cathode material for lithium ion batteries

Huanqiao Song[a, *], Yaguang Liu[a], Cuiping Zhang[a], Chaofeng Liu[a] and Guozhong Cao[a, b, *]

[a]Beijing Institute of Nanoenergy and Nanosystems, Chinese Academy of Sciences, Beijing 100083, China.

[b]Department of Materials and Engineering, University of Washington, Seattle, WA 98195-2120, USA

E-mail: songhuanqiao@binn.cas.cn; gzcao@u.washington.edu.

Supporting Information

The calculation of oxygen vacancies and true molecular formula for Mo doped LiV_3O_8 calcined at 400℃: The relative atomic ratio of V^{5+} and V^{4+} is 3:1 which was calculated based on the peak areas of V2p high resolution XPS. This means that the content of V^{4+} is 25% in vanadium ions and there are 0.71 V^{4+} per Mo doped LiV_3O_8 molecular. On the other hand, the substitution of a Mo^{6+} ion for a V^{5+} ion produces a V^{4+} ion, as dictated by the electroneutrality condition. 0.15 Mo^{6+} replaces V^{5+} in per molecular. The excess 0.56 V^{4+} come with the emergence of 0.28 oxygen vacancies. Therefore, the formula of Mo doped LiV_3O_8 is $LiMo_{0.15}V_{2.85}O_{7.72}(V_{\ddot{O}})_{0.28}$.

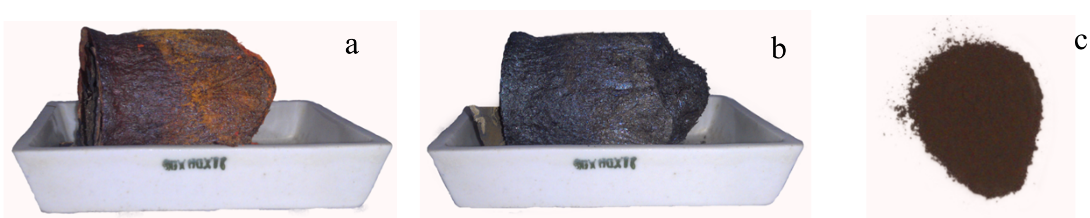

Figure S1 (a) Mo-doped LiV_3O_8 cryogel obtained by freeze drying. (b) Mo-doped LiV_3O_8 nanorod-assembled sheets obtained by annealing the cryogel in ambient atmosphere at 400℃ for 2 h. (c) Mo-doped LiV_3O_8 nanorod-assembled nanosheets obtained after ball milling.

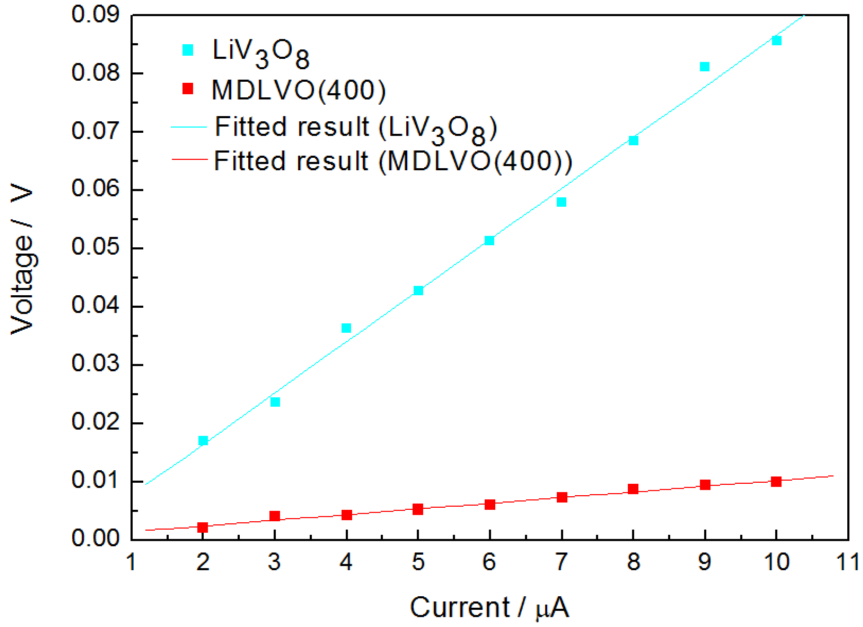

Figure S2 Current-voltage curves obtained by the DC four-probe measurements for LiV_3O_8 calcined at 400℃ and Mo-doped LiV_3O_8 (400) samples at room temperature.

Linear responses of the applied voltage range spectra were seen in Figure S2, which indicate that the electrical transports are within the ohmic region for LiV_3O_8 calcined at 400℃ and Mo-doped LiV_3O_8 (400) samples. The current (I) and voltage (V) in Figure S2 can be used to calculate the conductivity by the following expression

σ_{dc}= (I/V) (L/A) (S cm^{-1})

In above equation, L is the distance between the probes and A is the area of the sample. The electrical conductivity values were calculated to be $3.52 \times 10^{-6}\ S\ cm^{-1}$ and $2.89 \times 10^{-5}\ S\ cm^{-1}$ for LiV_3O_8 calcined at 400℃ and Mo-doped LiV_3O_8 (400) samples, respectively.

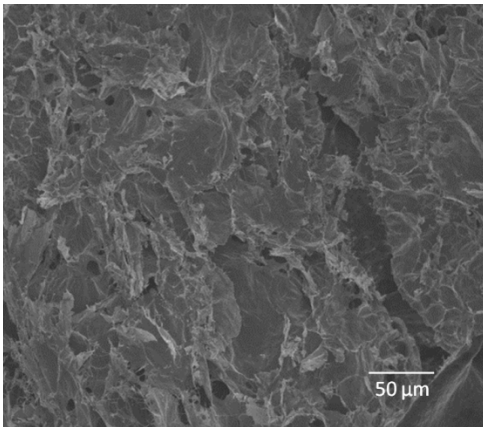

(a)

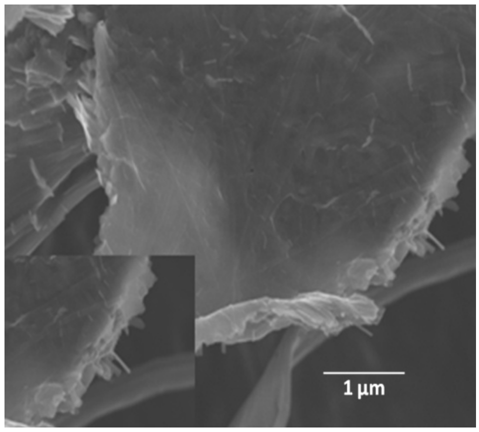

(b)

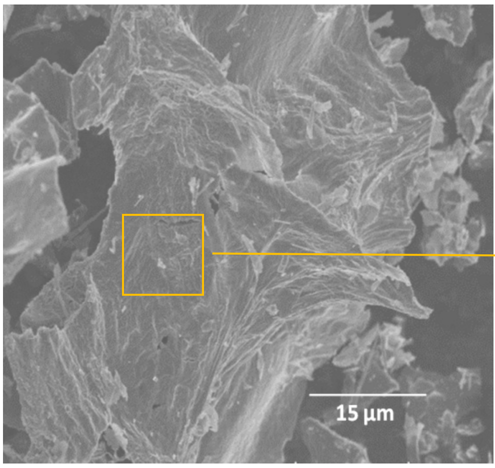

(c)

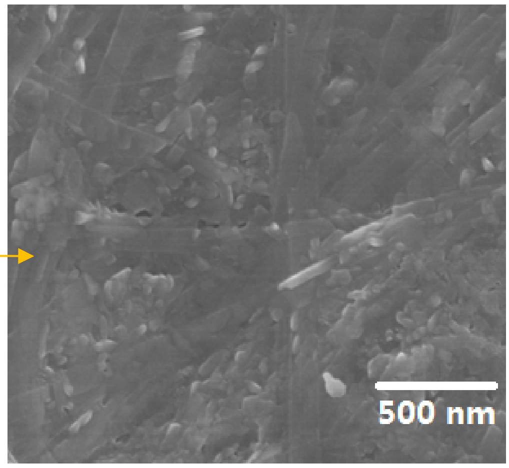

(d)

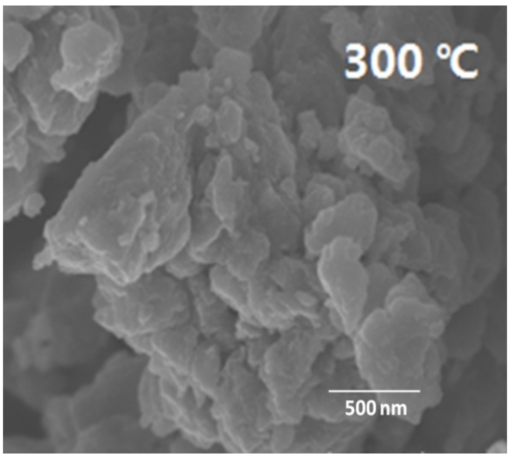

(e)

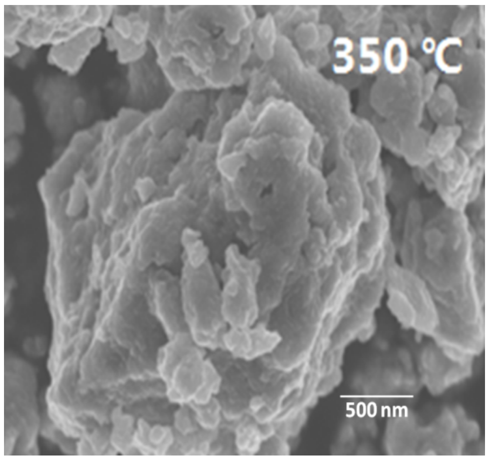

(f)

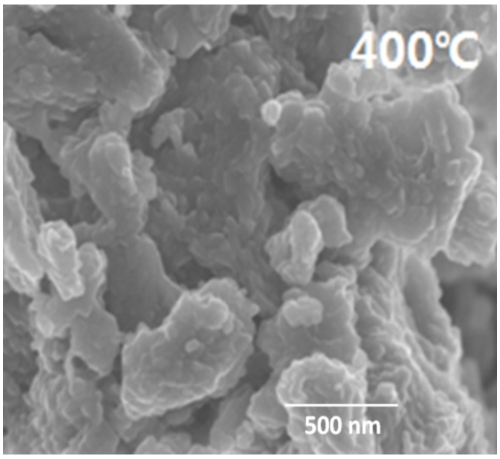

(g)

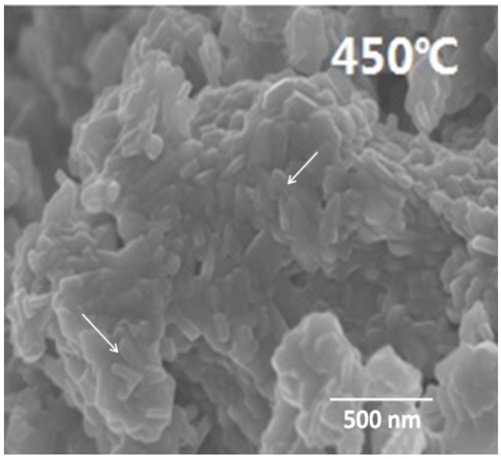

(h)

Figure S3 FE-SEM images of Mo-doped LiV_3O_8 cryogel (a, b), Mo-doped LiV_3O_8 calcined at 400 ℃ (c, d) and milled Mo-doped LiV_3O_8 calcined at 300℃ (e), 350℃ (f), 400℃(g) and 450℃ (h).

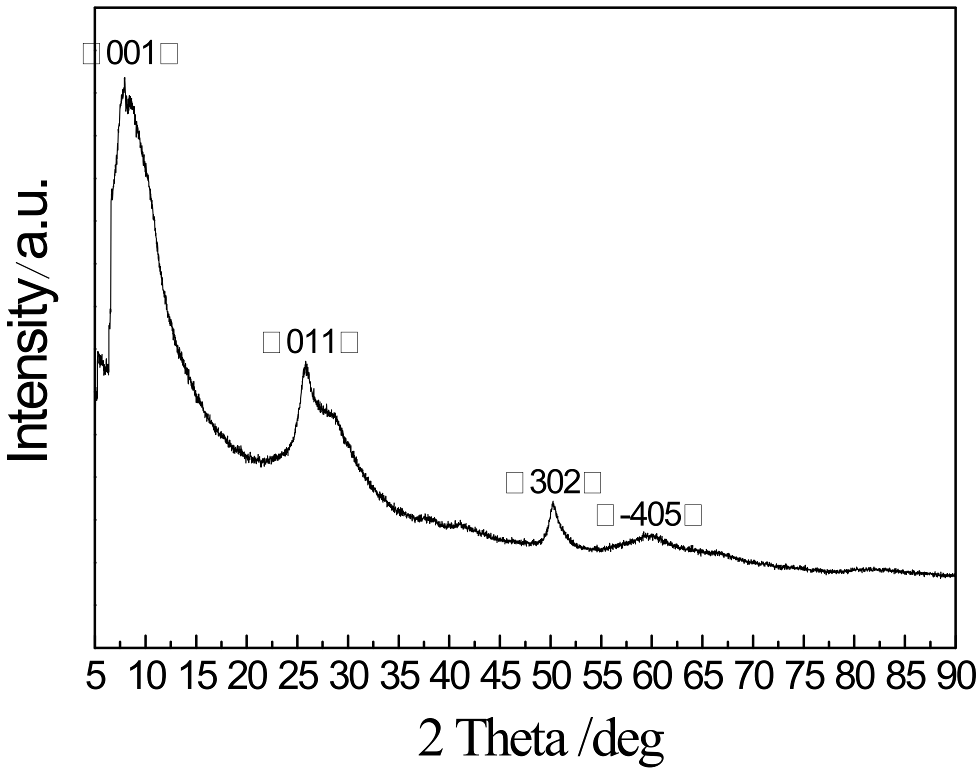

Figure S4 XRD pattern of milled Mo-doped LiV_3O_8 cryogel obtained by freeze drying.

The calculation of the NH_3 and O_2 partial pressure produced by the hydrothermal reaction: During the reaction, the volume of stainless steel autoclave is 100 ml, the amount of liquid is 60 ml and the V_2O_5 is 0.01mol. The number of moles of NH_3 and O_2 would be 0.0009 mol and 0.0003 mol based on the following formula.

$$28LiOH + 39.9V_2O_5 + 0.6(NH_4)_6Mo_7O_{24} \xrightarrow{180℃} 28LiMo_{0.15}V_{2.85}O_8 + 15.8H_2O + 3.6NH_3 \uparrow + 1.05O_2 \uparrow$$

The partial pressure of NH_3 and O_2 would be 113.02 Pa according to the ideal-gas equation, which is much smaller than the vapor pressure of water (1001900 Pa) and the pressure of air (153990 Pa) at 180 ℃. Therefore, the effects of NH_3 and O_2 were negligible on the total pressure in stainless steel autoclave.

$$PV = nRT$$
$$P = nRT / V$$
$$P = [(0.0009 + 0.0003) \times 8.314 \times (273.15 + 180)] / 0.04$$
$$P \approx 113.02(Pa)$$

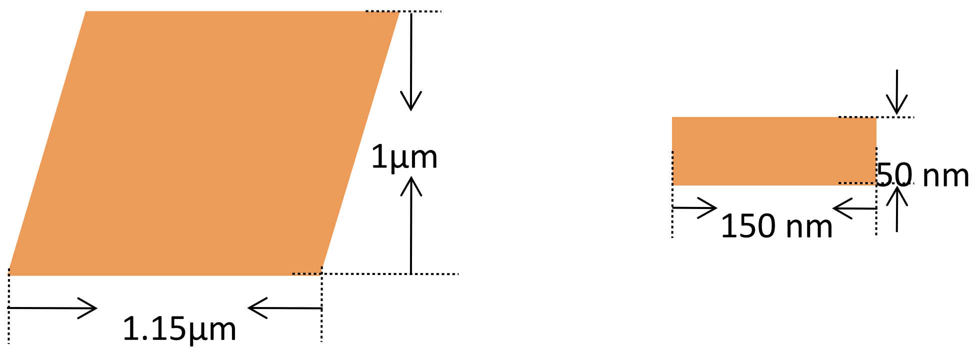

(a) (b)

Figure S5 Illustration of the calculation method to get the surface area of LiV_3O_8 (a) and MDLVO calcined at 400℃ (a, b).

The following is the calculation of LiV_3O_8 nanosheet surface area. The average length of LiV_3O_8 nanosheets is estimated to be 1.15 μm, the width and thickness are about 1 μm and 5 nm, respectively. The density of LiV_3O_8 is 3.48 g cm^{-3}. Therefore, the calculated surface area of LiV_3O_8 nanosheet is 116 m^2 g^{-1} based on the following equations.

$$S_S = 2 \times (L \times W + L \times T + W \times T) = 2 \times (1.15 \times 1 + 1.15 \times 0.005 - \times 10^{-12} = 2.32 \times 10^{-12} (m^2)$$

$$V = L \times W \times T = 1.15 \times 1 \times 0.005 \times 10^{-12} = 5.75 \times 10^{-15} (cm^3)$$

$$m_S = \rho V = 3.48 \times 5.75 \times 10^{-15} \approx 2.00 \times 10^{-14} (g)$$

$$S_T = {S_S}/{m_S} = {2.32 \times 10^{-12}}/{2.00 \times 10^{-14}} = 116 (m^2\ g^{-1})$$

Gas-adsorption derived surface area (13.9 m^2 g^{-1}) occupies only 11.98% of the calculated surface area. That is, only 11.98% of the calculated surface area can be in contact with the electrolyte supposing all of the LiV_3O_8 are nanosheets.

As for the Mo-doped LiV_3O_8 material calcined at 400℃ (MDLVO (400)), its structure comprises of nanorod-assembled nanosheets. The calculation surface area is as follows supposing all of the MDLVO (400) are nanorods. The average length of the MDLVO (400) nanorods is estimated to be 150 nm, the width is 50 nm and the thickness is about 5 nm. The nanorod is assumed to be cuboid. Therefore, the calculated surface area of LiV_3O_8 nanorod is 131 m^2 g^{-1} based on the following equations.

$$S = 2 \times (L \times W + L \times T + W \times T) = 2 \times (150 \times 50 + 50 \times 5 + 150 \times 5) \times 10^{-18} = 1.70 \times 10^{-14} (m^2)$$

$$V = L \times W \times T = 150 \times 50 \times 5 \times 10^{-21} = 3.75 \times 10^{-17} (cm^3)$$

$$m_S = \rho V = 3.48 \times 3.75 \times 10^{-17} \approx 1.30 \times 10^{-16} (g)$$

$$S_T = {S_S}/{m_S} = {1.70 \times 10^{-14}}/{1.30 \times 10^{-16}} \approx 131 (m^2 g^{-1})$$

Gas-adsorption derived surface area (24.8 m^2 g^{-1}) occupies 18.93% of the calculated surface area, and the corresponding ratio of calculated surface area can be in contact with the electrolyte. The ratio of active surface area increases 58.01% comparing with LiV_3O_8 nanosheets.

If all of the MDLVO (400) are nanosheets, the gas-adsorption derived surface area (24.8 m^2 g^{-1}) would take 21.38% of the calculated surface area. And the ratio of active surface area would increase 78.46% comparing with that of LiV_3O_8 nanosheets. Collectively, the BET surface area has increased 78.42% after Mo doped LiV_3O_8 nanosheets and the ratio of active surface area has also an increase of 58.01%-78.46% comparing with that of LiV_3O_8 nanosheets. Therefore, the different electrochemical performance would be obtained due to the doping of Mo.

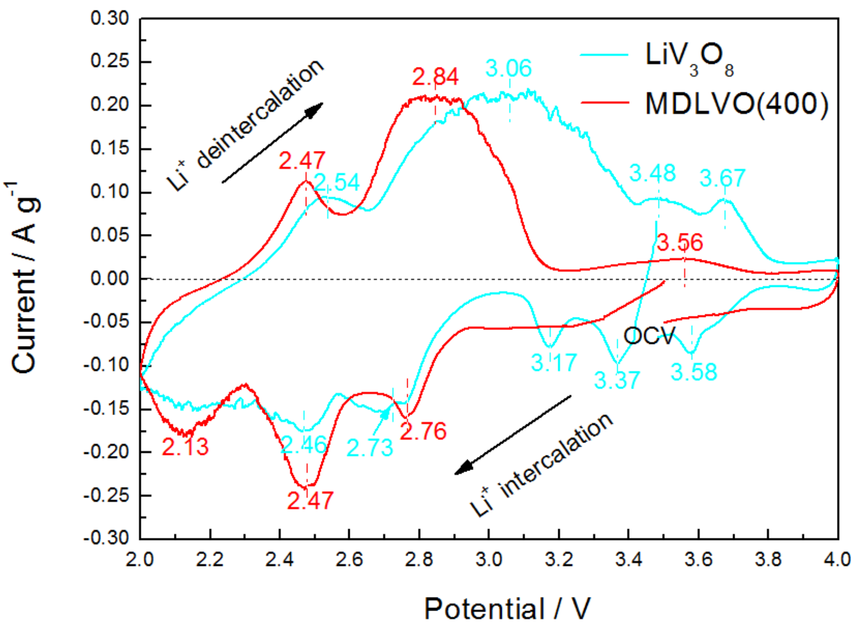

Figure S6 The first-cycle CV curves for pure LiV_3O_8 calcined at 400℃ and Mo-doped LiV_3O_8 (400) electrodes at a scan rate of 0.1 mV s^{-1} over the range of 2.0-4.0 V (*vs.* Li/Li^+).

Table S1. Impedance parameters calculated from equivalent circuit.

	R_s(Ω)	R_f(Ω)	R_{ct}(Ω)
LiV_3O_8	4.3	134.2	155.2

MDLVO(400)	1.9	59.6	68.1

Table S2. BET surface areas of Mo-doped LiV_3O_8 samples calcined at different temperatures.

Samples	MDLVO(300)	MDLVO(350)	MDLVO(400)	MDLVO(450)
BET/ m^2 g^{-1}	29.5	27.3	24.8	16.9

Table S3. Comparison of electrochemical performance of different LiV_3O_8 electrode materials.

Electrode material	The highest capacity ($mA\ h\ g^{-1}$)	Capacity after cyclings ($mA\ h\ g^{-1}$)	Reference
Mo doped LiV_3O_8	4-2 V: 269.0 at 300 mA g^{-1}	205.9 after 100 cycles	This work
Pure LiV_3O_8	4-2 V: 292.0 at 300 mA g^{-1}	97.8 after 100 cycles	This work
LiV_3O_8 nanorods on graphene	4-1.5 V: ~ 226 at 300 mA g^{-1}	~197 after 100 cycles	Ref [1]
$Li_xV_2O_5/LiV_3O_8$ nanoflakes	4-1.5 V: 195.4 at 300 mA g^{-1}	163.4 after 200 cycles	Ref [2]
Al_2O_3 coated LiV_3O_8	4-2 V: 283.1 at 100 mA g^{-1}	205.7 after 100 cycles	Ref [3]
LiV_3O_8/polythiophene	4-1.8 V: ~255 at 300 mA g^{-1}	216.7 after 50 cycles	Ref [4]
LiV_3O_8 nanosheets	4-1.5 V: 232.4 at 300 mA g^{-1}	~195 after 100 cycles	Ref [5]
Al_2O_3-modified LiV_3O_8	4-1.5 V: ~200 at 300 mA g^{-1}	191.0 after 200 cycles	Ref [6]

References

[1] R. Mo, Y. Du, N. Zhang, D. Rooney, K. Sun, Chem. Commun. 49 (2013) 9143-9145.

[2] D. Sun, G. Jin, H. Wang, X. Huang, Y. Ren, J. Jiang, H. He, Y. Tang, J. Mater. Chem. A 2 (2014) 8009-8016.

[3] S. Huang, J.P. Tu, X.M. Jian, Y. Lu, S.J. Shi, X.Y. Zhao, T.Q. Wang, X.L. Wang, C.D. Gu, J. Power Sources 245 (2014) 698-705.

[4] H. Guo, L. Liu, H. Shu, X. Yang, Z. Yang, M. Zhou, J. Tan, Z. Yan, H. Hu, X. Wang, J. Power Sources 247 (2014) 117-126.

[5] H. Wang, Y. Ren, Y. Wang, W. Wang, S. Liu, CrystEngComm 14 (2012) 2831-2836.

[6] R. Mo, Y. Du, N. Zhang, D. Rooney, K. Sun, J. Power Sources 257 (2014) 319-324.